

A GENERAL METHOD FOR ASSESSING THE ORIGIN OF INTERSTELLAR SMALL BODIES: THE CASE OF 1I/2017 U1 (OUMUAMUA)

JORGE I. ZULUAGA, OSCAR SÁNCHEZ-HERNÁNDEZ, MARIO SUCERQUIA & IGNACIO FERRIN
Solar, Earth and Planetary Physics Group & Computational Physics and Astrophysics Group (FACOM)
Instituto de Física - FCEN, Universidad de Antioquia, Calle 67 No. 53-108, Medellín, Colombia

Draft version October 9, 2018

ABSTRACT

With the advent of more and deeper sky surveys, the discovery of interstellar small objects entering into the Solar System has been finally possible. In October 19, 2017, using observations of the PANSTARRS survey, a fast moving object, now officially named 1I/2017 U1 (Oumuamua), was discovered in a heliocentric unbound trajectory suggesting an interstellar origin. Assessing the provenance of interstellar small objects is key for understanding their distribution, spatial density and the processes responsible for their ejection from planetary system. However, their peculiar trajectories place a limit on the number of observations available to determine a precise orbit. As a result, when its position is propagated $\sim 10^5 - 10^6$ years backward in time, small errors in orbital elements become large uncertainties in position in the interstellar space. In this paper we present a general method for assigning probabilities to nearby stars of being the parent system of an observed interstellar object. We describe the method in detail and apply it for assessing the origin of 1I/2017 U1. A preliminary list of potential progenitors and their corresponding probabilities is provided. In the future, when further information about the object and/or the nearby stars is refined, the probabilities computed with our method can be updated. We provide all the data and codes we developed for this purpose in the form of an open source C++/Python package, *iWander* which is publicly available at <http://github.com/seap-udea/iWander>.

Subject headings: Interstellar small body — asteroids: individual: 1I/2017 U1 — Methods: numerical

1. INTRODUCTION

The detection of interstellar small objects, wandering through the Solar System, has challenged the astronomers over the last century (see eg. [Opik 1932](#); [McGlynn & Chapman 1989](#); [Sen & Rama 1993](#)). The detection, characterization and investigation of the origin of these objects could shed light on the processes of planetary formation, the architecture of their parent planetary systems, as well as on planetary ejection mechanisms. Moreover, interstellar visitors can also be the target for future exploration missions (the first ones traveling to an interstellar object; [Mamajek 2017](#)), become an indirect way to detect planetary systems of nearby stars and to infer some of their properties ([Trilling et al. 2017](#)) or help to test bold hypotheses about the origin and distribution of life in the Universe, such as lithopanspermia ([Adams & Spergel 2005](#); [Belbruno et al. 2012](#)).

Recently, [Engelhardt et al. 2017](#) calculated the number density of detectable interstellar objects, obtaining a discouraging value of $1.4 \times 10^{-4} \text{ au}^{-3}$ which seemed to restrict severely the chances of detecting one of these objects in the coming years, at least with the current available instrumentation. Nevertheless, on 19 October 2017 a small object with an uncommon orbit ($e = 1.19 \pm 0.007$ and $v_\infty = 26.2 \pm 0.1 \text{ km/s}$) was discovered using the PANSTARRS Survey ([Chambers et al. 2016](#)). The orbital properties that were determined using a short orbital arc, while the object was still visible after their rapid passage through perihelion, suggested an interstellar origin. This result was supported by follow-up spectroscopic observations ([Bolin et al. 2017](#)) and other theoretical considerations ([Ye et al. 2017](#); [Masiero 2017](#)). The

interloper object has been now named “1I/Oumuamua” or alternatively “1I/2017 U1” as we will call it consistently through this paper¹.

The first follow-up observations suggested that the object was of asteroidal origin, and its composition seemed to be similar to that of transneptunian objects (TNOs) ([Merlin et al. 2017](#)). More recently, [Jewitt et al. \(2017\)](#) measured the observed color and suggested a composition overlapping the mean colors of D-type Trojan asteroids and other inner solar system populations, but inconsistent with the ultra-red matter found in the Kuiper belt. [Ferrin & Zuluaga \(2017\)](#) compared the color of the object with other 21 active and extinct Solar System comets and suggest that 1I/2017U1 could actually be an inactive extrasolar comet. This result could be very important for assessing their dynamical origin.

Only a few days after the announcement of the discovery, several works attempting to pinpoint its interstellar origin were published in the form of research notes and short papers ([Mamajek 2017](#); [de la Fuente Marcos & de la Fuente Marcos 2017](#); [Gaidos et al. 2017](#); [Portegies Zwart et al. 2017](#); [Dybczyński & Królikowska 2017](#)). Most of these initial works were able to restrict the origin of the object to nearby stars and young planetary systems from which it could have escaped via planet-planet scattering. These early attempts, however, either rely on rough comparisons between the heliocentric entrance velocity of the object and that of nearby stars ([Mamajek 2017](#); [Gaidos et al. 2017](#)) and/or on the numerical propagation of the orbit of the object among many nearby stars, in the galactic potential ([Portegies Zwart et al. 2017](#);

¹ IAU Minor Planet Center, 2017, U183

Dybczyński & Królikowska 2017). These latter efforts, however, lack of a rigorous consideration of the orbit uncertainties and the errors in the astrometric and radial velocities of the stars. Several authors have even suggested that given the current orbital uncertainties and astrometric information about nearby stars, pinpointing the exact origin of 1I/2017U1 (and possibly other future interstellar objects) to a specific stellar system could be impossible.

The detection of 1I/2017U1 however, allowed some authors to update estimations of the number densities of interstellar objects and their detection probability. Thus, for instance, Trilling et al. 2017 recently determined that if during planet formation processes the ejected mass was about 20 Earth’s masses, the detection rate of such interstellar objects could be at least 0.2 per year with the current instrumentation. This result is consistent with the discovery of 1I/2017U1 this year. Moreover, when the Large Synoptic Survey Telescope (LLST, Ivezić et al. 2008) begins its wide, fast and deep all-sky survey the rate could climb to 1 per year. As a result, developing a general and rigorous strategy for assessing the origin of this and probably other objects detected in the future, is an important goal to pursue.

The problem of tracking small Earth’s impactors towards their progenitor objects in the Solar System has been extensively studied in the literature (see e.g. Strom et al. 2005; Zuluaga et al. 2013; Strom Robert et al. 2015; Zuluaga & Sucerquia 2017). However, the dynamic of the Solar System is well constrained. The timescales are relatively short and the the position of the perturbing objects is known to exquisite levels of precision. This is not the case when reconstructing the orbit of an interstellar object. Timescales are huge amplifying even small uncertainties in initial positions. The perturbing objects (stars) are very distant and small errors in their projected position in the sky correspond to large errors in their position in space. With the advent of precise astrometric missions such as Gaia, the situation is improving significantly, but has not been solved.

Tracking the motion of objects in the interstellar space is not new. Several authors have studied the problem, aimed to determine the past and future close encounters of the Sun with nearby stars (See e.g. García-Sánchez et al. 2001; Bailer-Jones 2015; Berski & Dybczyński 2016). Of particular interest for this work is the recent paper by Bailer-Jones (2017) which use up-to-date astrometric and radial velocity catalogs to study this problem, while rigorously considering the uncertainties involved. This work is inspired and mostly based on the models, data and techniques developed in that work.

In this paper we present a general methodology and a computer tool designed for assessing the dynamical origin of an interstellar object. Instead of determining which particular stellar system could be the source of a given object, the methodology presented here aims at computing the “interstellar origin probabilities” (hereafter IOP) of many nearby stars. For that purpose it takes into account rigorously the uncertainties in the initial observations. When more and better astrometric information become available, the IOP can be improved.

This paper is organized as follows: in section 2 we outline the method. Sections 3, 4 and 5, 6 present the details of the implementation, while illustrating each technique

in the particular case of 1I/2017U1. Section 8 defines the concept of “Interstellar Origin Probability”. The results of applying the methodology to the case of 1I/2017U1 are presented in section 9 including a list of the potential progenitors with their respective IOP. Finally, section 11 is devoted to discussing the limitations of the method, but also its future potential as a general framework to study the orbit of discovered objects.

2. OUTLINE OF THE METHOD

Once a small body is discovered in the Solar System, the up-to-date best-fit orbital solution for the object is published by the Minor Planet Center (MPC), and it is made available publicly, for instance, in the JPL Small-Body Database Browser². The orbit solution is provided in the form of a vector of “nominal orbital elements” $E_0 : (e_0, q_0, t_{p,0}, \Omega_0, \omega_0, i_0)$ (orbital eccentricity, perihelion distance, time of perihelion passage, longitude of the ascending node, argument of the perihelion and inclination, respectively) at a reference epoch t_0 . Along with this information, the MPC provides also the nominal mean orbital motion n_0 , and its standard errors σ_{n_0} . The uncertainties in the orbital fit are characterized with an “orbit covariance matrix”, C_{jk} , defined as:

$$C_{jk} = \begin{cases} \sigma_j^2 & j = k \\ \rho_{jk}\sigma_j\sigma_k & j \neq k \end{cases} \quad (1)$$

where $j : e, q, t_p, \Omega, \omega, i$ and ρ_{jk} are the correlations among the orbital elements.

The question we seek to solve in this paper is if given this initial orbital information, in particular in the case of an unbound object ($e_0 > 1$), there exists an efficient method to compute the probability that a given star, whose position in the sky and velocity in space is known only approximately, be the progenitor of the small body.

In the following paragraphs we outline the method we devised to solve the origin problem of interstellar objects. The details of the method and the theory behind it are presented in the following sections. Of course the method is not completely original and has its roots in preceding works, particularly on those of Zuluaga & Sucerquia (2017) and Bailer-Jones (2015, 2017).

2.1. The method

1. Generate N_p clones of the orbital elements vector E , compatible with the latest orbital solution E_0 and C_{jk} (see section 3). These clones describe the orbit of what we will call the “surrogate objects” (following the convention of Bailer-Jones 2017).
2. Integrate backwards the orbits of the surrogate objects, until a time when the object in the nominal orbit reaches a distance from the Sun where the galactic tides become relevant for the dynamic of the object (see section 4).
3. Using the “linear motion approximation” (LMA), identify the stars in an astrometric and radial velocity catalog, such that their minimum distance to the nominal object, $d_{LMA,\min}$, be less than or

² <https://ssd.jpl.nasa.gov/>

equal to a threshold distance $D_{\max,1}$. Stars identified with this procedure are called the “candidates” (see [section 5](#)).

4. For each candidate, compute a more precise encounter time t_{\min} and minimum distance d_{\min} by integrating the orbit of the star and the nominal object in the galactic potential (see [section 6](#)).
5. Identify those candidates for which the more precisely computed minimum distances is below a tighter distance threshold $D_{\max,2}$. We call these the “potential progenitors”.
6. For each potential progenitor, generate N_s “surrogate stars” (hypothetical stars having astrometric properties compatible with the observed properties of the star and their errors). For each surrogate star, calculate the “interstellar origin probability” (IOP), roughly defined as the probability that the object had the same position as the surrogate and a relative velocity of a magnitude compatible with the expected ejection mechanisms. The probability is “corrected” by the present distance of the object to the surrogate star and with the probability that it can be ejected from a different potential progenitor (see [section 8](#)).

All the potential candidates identified with this procedure are tabulated in descending order of IOP probability ([Table 4](#)). The idea is not to select an individual star (or none), but to assign a probability to the star, that can be improved with this method as the object and the star are better known.

3. THE SURROGATE OBJECTS

Since the trajectory of the object is uncertain, and small errors inside the Solar System amplify when the orbit is integrated into the interstellar space, we cannot rely on a single orbit (the nominal solution) for assessing its interstellar origin.

Instead we generate N_p vectors of orbital elements E compatible with the orbital solution described with E_0 and C_{jk} (see [section 2](#)). For this purpose we use a multivariate gaussian random number generator³, having mean values equal to the nominal solution element vector E_o and covariance, equal to the orbit covariance.

In [Figure 1](#) we show a particular realization of the orbital elements for the surrogate objects of 1I/2017U1 generated with this procedure. Given the strong correlation between the orbital elements, most of the surrogate objects have elements located in a very elongated ellipsoid in configuration space. To better illustrate the method and obtain conservative estimates of the IOP probabilities, we will assume hereafter that the orbital elements, instead of following the original orbit covariance (top panel in [Figure 1](#)) are related through a diagonal version of the matrix, such that where $\rho_{jk}=0$ (bottom panel in [Figure 1](#)).

³ Most numerical libraries are provided with a multivariate random number generator. In the particular case of this work we use the generator and related routines provided by the GNU Scientific Library GSL ([Galassi et al. 2002](#))

4. TRAJECTORY IN THE SOLAR SYSTEM

Once the orbital elements of the surrogate objects have been generated at the reference epoch, we proceed to calculate the trajectory of each object in the gravitational field created by the sun and the 8 planets⁴.

For that purpose we use a Gragg-Bulirsch-Stoer algorithm ([Gragg 1965](#); [Bulirsch & Stoer 1966](#)) adapted from [site](#)⁵. Positions and velocities of the the planets were not computed with the integrator itself, but taken directly from the latest DE431 planetary kernel and using NASA NAIF SPICE ([Acton Jr 1996](#) and [Jon D. Giorgini](#))⁶. We verified that for the case of 1I/2017U1, our integrations were close to the precise solutions computed by the JPL group and published in the on-line NASA Horizons system, within 0.1% at least back to 400 years before the reference epoch.

Since the trajectory of the object is hyperbolic, and in the case of 1I/2017U1, highly inclined with respect to the ecliptic ($i=122.6^\circ$), the object reached large distances to the Sun and the planets in relatively short times. Given the original uncertainty in the orbit, using the integrator to compute a very precise position of the surrogate objects within the Solar System is pointless. At some time in the past, the accumulated errors in the state vector (x, y, z, v_x, v_y, v_z) due only to the orbit uncertainty, will be much larger than the errors from assuming that the objects move in an ideal hyperbola.

Thus, for instance, in the case of 1I/2017U1, we verified that at $t = -100$ years, the positions of the surrogate objects were spread inside an ellipsoid with a characteristic size of 2-3 AU (see [Figure 2](#)). On the other hand, the osculating elements of the object orbit at $t = -0.6$ years, when it was at only at 3 AU from the Sun and above the ecliptic plane, allows us to predict the position at $t = -100$ years with an uncertainty of $\sim 0.2-0.3$ AU. We call the orbital elements at this critical point, the “asymptotic elements” and use them to compute the position of the object in the far past. The value of the asymptotic elements for 1I/2017U1 are presented in [Table 1](#).

Using the asymptotic orbital elements we calculate the position and velocity of the surrogate objects at arbitrary times in the past. However, when the object is at a distance comparable with the truncation tidal radius of the Solar System, $d_{T,\odot}$, the effects of the galactic potential in its motion cannot be neglected. We call this epoch the “time of ingress” t_{ing} . The interstellar orbit integration for the surrogate objects and stars start at t_{ing} . In [Table 1](#) we show the time of ingress for 1I/2017U1 and its position and velocity in the ICRS galactic reference frame at that time. Our results are in agreement to those of [Mamajek \(2017\)](#).

In order to illustrate the effect that uncertainties in the orbit solution has in the predicted position of the object in the past, we show in [Figure 2](#) the radiant in the sky of the surrogate objects at ingress time. We also plot the position in space of the objects in the ICRS galactic reference frame, their velocities in the same reference frame

⁴ Although dwarf planets and major asteroids were not included in the integrations presented here, it is easy to add them in the `iWander` package provided with this work

⁵ <http://www.mymathlib.com/>

⁶ <http://naif.jpl.nasa.gov/pub/naif>

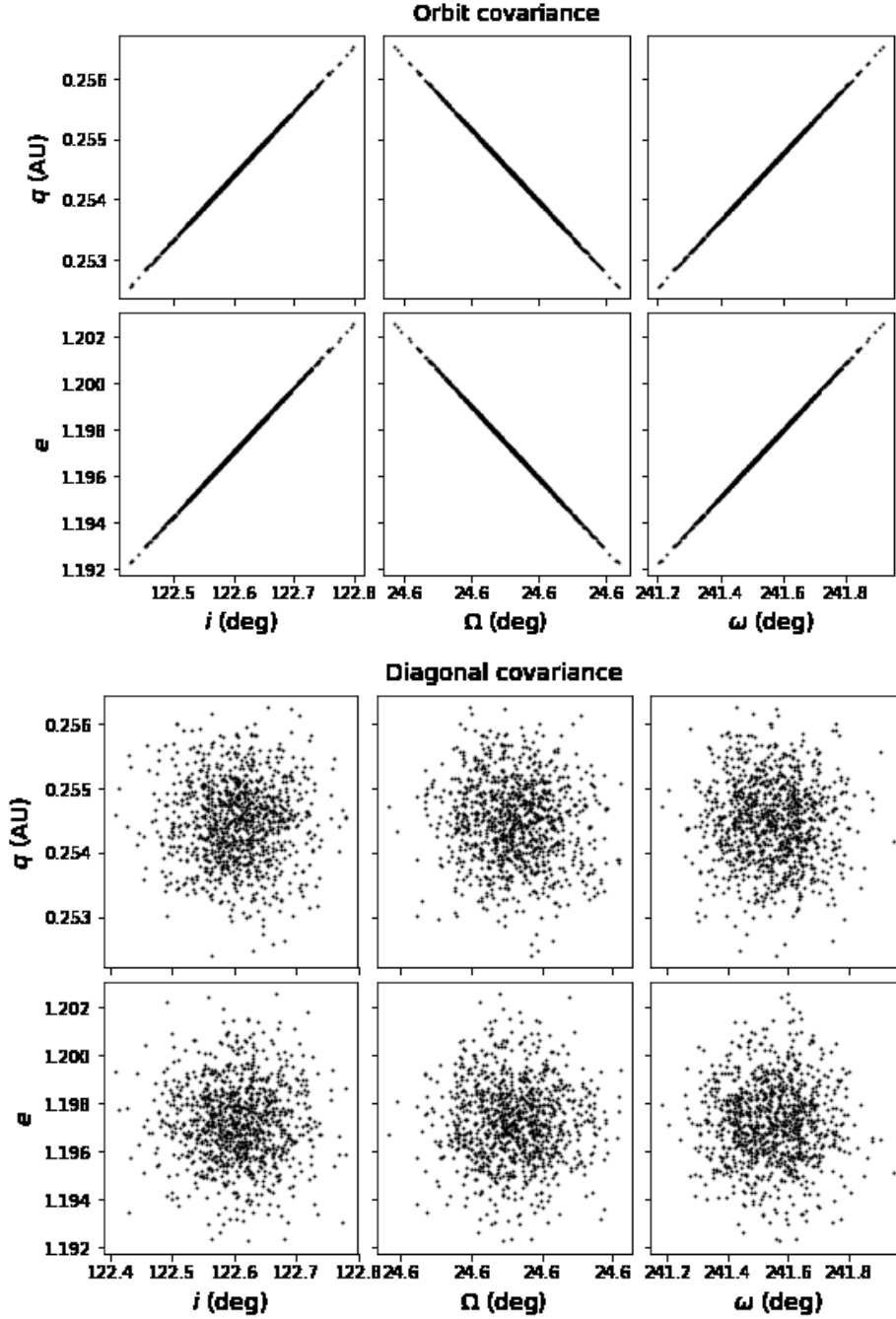


FIG. 1.— Top panel: Elements of the 1000 surrogate objects for 11/2017U1, generated assuming the nominal solution and orbit covariance provided by the MPC. Bottom panel: orbital elements generated assuming a diagonal orbit covariance (no correlation). The second set of surrogate objects are used for illustration purposes and to obtain a conservative estimation of the IOP. For brevity we have not included here, the panels corresponding to the perihelion passage t_p , and other correlations such as that of Ω - ω .

Property	Value
Reference Epoch	2458052.5 TDB = October 26.0 2017
Nominal elements	$q = 0.2544567273$ AU $e = 1.1971887090$ $i = 122.6040164923$ deg $\Omega = 24.6029592566$ deg $\omega = 241.5429238264$ deg $M = 31.2832803597$ deg $\mu = 1.3271244002 \times 10^{11}$ km ³ /s ²
Epoch of Asymptotic elements	2457847.96 TDB = April 4.46 2017
Asymptotic elements	$q = 0.2512935611$ AU $e = 1.1946156513$ $i = 122.6602032110$ deg $\Omega = 24.2202949461$ deg $\omega = 241.5291945547$ deg $M = -69.1715435532$ deg $\mu = 1.3271244002 \times 10^{11}$ km ³ /s ²
Truncation radius	10^5 AU
Time of ingress	-1.81×10^4 years
Radiant at ingress	RA = 280.15 ± 0.20 deg DEC = 34.15 ± 0.07 deg $l = 63.17 \pm 0.11$ deg $b = 16.9 \pm 0.14$ deg
Velocity at ingress	U = -11.316 ± 0.078 km/s V = -22.378 ± 0.077 km/s W = -7.617 ± 0.087 km/s

TABLE 1
PROPERTIES OF THE ORBIT OF 11/2017U1 IN THE SOLAR SYSTEM

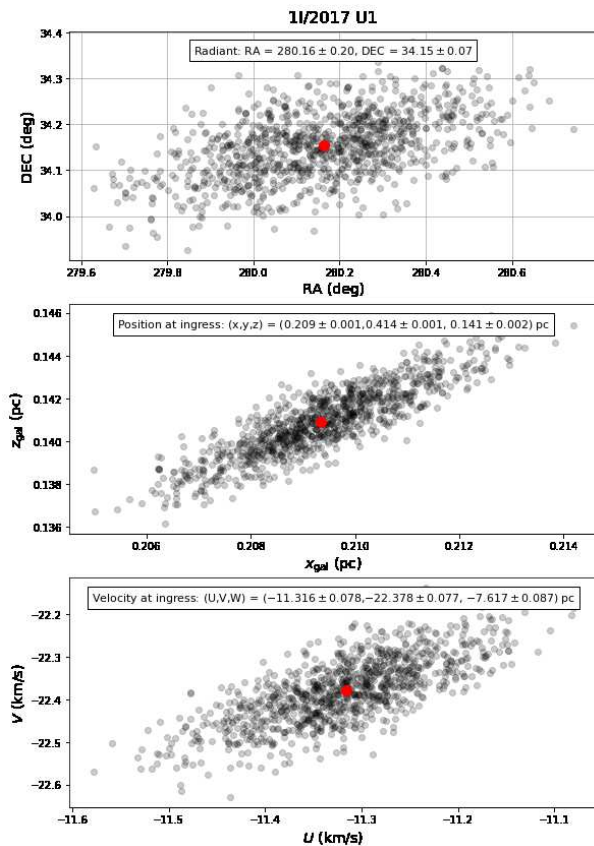


FIG. 2.— Dispersion in the position of the surrogate objects at the time of ingress into the Solar System. Right ascension, RA and declinations, DEC are referred to the Solar System Barycenter and the J2000 equinox. Galactic cartesian coordinates $(x_{gal}, y_{gal}, z_{gal})$ and velocities (U, V, W) are referred to the ICRS galactic system of reference.

and their corresponding errors. The convention stands that (U, V, W) correspond to $(v_{gal,x}, v_{gal,y}, v_{gal,z})$.

As commented before, even a small error in the orbital elements at the reference epoch are propagated as relatively large errors at the ingress time. While at $t = -100$ yrs the dispersion was of 2-3 AU, at t_{ing} the surrogate objects have spread as a ~ 0.04 pc cloud. We have verified that this trend continues into the interstellar space, with a growing rate of ~ 0.25 km/s (the “size” of the cloud in the velocity UVW space, see bottom panel in Figure 2). At this rate, the cloud characteristic size will grow to ~ 2 pc (the typical distance between stars in the solar neighborhood) in ~ 10 Myr. Beyond this time, several particles in the cloud of surrogate objects will always cross at least one nearby star, and the reliability of our method will be compromised. We call this the “maximum retrospective time”, t_{ret} . In the case of 11/2017U1 and as argued before, $t_{ret} \sim 10^7$ yrs

5. ASTROMETRIC AND RADIAL VELOCITY DATABASES

In order to compare the position of our interstellar object with the position of nearby stars in the far past, we need to know as precisely as possible the position and velocities of those stars at present time. For this purpose we have compiled up-to-date astrometric information (position, parallaxes, proper motion and radial velocities) of 267,968 stars (see Table 2).

Compiling precise astrometric and radial velocity measurements for a significant number of nearby stars, is tricky. On one hand, precise astrometric databases such as Hipparcos (Perryman et al. 1997) and Tycho-2 (Høg et al. 2000) does not include radial velocities measurements. The Gaia mission have the potential to provide this information, but it will only be available since Data Release 2 (DR2) in April 2018⁷.

On the other hand, there are several public catalogs that provide precise radial velocities (see Table 2). However, not all the objects in those catalogs are included in the astrometric catalogs, and in some cases they have unique identifications without any reference to the Hipparcos/Tycho-2 ids, which are to the date of writing this paper, the identification for objects having precise astrometric measurements (either from the Hipparcos or the Gaia mission).

We compile the information required for this work following the detailed directions recently published by Bailer-Jones 2017. Additionally, and in order to include nearby bright stars (which were not included in the Gaia catalog) we search for other information about the Hipparcos stars in the Simbad information system⁸.

The importance of having this information centralized and updated led us to create a catalog we called the AstroRV catalog (astrometric and radial velocities). The catalog is provided with the iWander package developed in this work.

For the sake of completeness and reproducibility we outline below the procedure required to create the AstroRV catalog:

1. Get available astrometric and radial velocities catalogs. In Table 2 we summarize the information

⁷ <https://www.cosmos.esa.int/web/gaia/release>

⁸ <http://simbad.u-strasbg.fr/simbad/>

of the catalogs we use for this work. The most important one is the Gaia DR1 catalog containing 2,057,050 objects. Of them 93,635 are also in the Hipparcos catalog and 1,963,415 are in the Tycho-2 catalog (Brown et al. 2016).

2. Obtain the general information available in *Simbad* for all the stars having an Hipparcos ID. The information includes other designations for the stars (Henry Draper catalog id and proper names for the bright stars) and radial velocities for some of those stars.
3. Find all the objects in the Hipparcos and Tycho Catalogues (ESA 1997) and in the Simbad table compiled before, that are not included in the GAIA DR1 catalog. Append the resulting objects to the latest catalog to create a final table with all the available astrometric information. We call the resulting list the *Astro* catalog.
4. Create a table including all objects in the radial velocities catalogs that have Hipparcos and/or Tycho-2 ids. For those objects not having any of those ids, find the Hipparcos/Tycho-2 objects matching the coordinates within a 50 arcsec radius (we use for this purpose the X-match tool of *Simbad*). The resulting table is called the *RV* catalog. For detailed instructions about how to compile radial velocities please refer to Bailer-Jones (2017).
5. Merge the *Astro* and *RV* catalog according to the Hipparcos/Tycho-2 ids. The resulting table is the *AstroRV* catalog.

The catalog created with this procedure contains 244,589 stars including the nearest and brightest ones. We provide with the *iWander* package the required scripts for creating the catalog as described before. This scripts can be modified to include future radial velocity and astrometric catalogs, or to update the information in older versions. An up-to-date version of the *AstroRV* catalog will be available at the *iWander* GitHub repository⁹.

6. TRAJECTORIES IN INTERSTELLAR SPACE

Having the position and velocity of both, the surrogate objects and the nearby stars, we now may integrate their orbits backward in time to identify any close approach. Since we need to perform a comparison between the position of at least $\sim 1,000$ surrogate objects with $\mathcal{O}(10^5)$ stars, computing times may become prohibitively large. In a first step we perform a selection of stellar candidates using the so-called “linear motion approximation” (LMA).

6.1. The LMA approximation

Under this approximation all particles, the surrogate objects and the stars, move in straight lines:

$$\vec{r}_i(t) = \vec{r}_{i,0} + \vec{v}_{i,0}t$$

The instantaneous distance between objects j and k , is then given by:

$$\begin{aligned} |\Delta\vec{r}_{jk}(t)|^2 &= |\Delta\vec{r}_{jk,0} + \Delta\vec{v}_{jk,0}t|^2 \\ &= \Delta\vec{r}_{jk,0}^2 + 2\Delta\vec{r}_{jk,0}\Delta\vec{v}_{jk,0}t + \Delta\vec{v}_{jk,0}^2t^2 \end{aligned}$$

where $\Delta\vec{r}_{jk,0} = \vec{r}_{k,0} - \vec{r}_{j,0}$ and $\Delta\vec{v}_{jk,0} = \vec{v}_{k,0} - \vec{v}_{j,0}$. This function is minimum when $d|\Delta\vec{r}_{jk}(t)|^2/dt = 0$, ie. at the time $t_{jk,\min}$ when the distance between the objects is $d_{jk,\min}$:

$$\begin{aligned} t_{jk,\min} &= \Delta\vec{r}_{jk,0} / \Delta\vec{v}_{jk,0} \\ d_{jk,\min} &= \Delta\vec{r}_{jk}(t_{\min}) \end{aligned} \quad (2)$$

We compute $t_{jk,\min}$ and $d_{jk,\min}$ for the nominal object and all the stars in our *AstroRV* in order to select the candidate stars.

For the next step, that involves computationally expensive tasks, we select from the catalog only the stars that fulfill $d_{jk,\min} < D_{\max}$, with D_{\max} defined as a piecewise function of the initial heliocentric distance of the star d_0 :

$$D_{\max}(d_0) = \begin{cases} d_0/10 & d_0 < 10 d_{\max} \\ d_{\max} & \text{otherwise} \end{cases} \quad (3)$$

This definition is intended to avoid that all the stars at distances below d_{\max} be selected independent of their kinematical properties. For the case of II/2017U1 we found that $d_{\max} = 50$ pc is a good threshold value to filter out stars potentially having a close encounter with the object.

For each “candidate” star selected with the preceding criterion, we should convert their observed properties (RA, DEC, $\varpi, \mu_\alpha, \mu_\delta, v_r$) (right ascension, declination, parallax, projected proper motion in RA, proper motion in declination and radial velocity, respectively) into its spatial cartesian coordinates in the galactic system, $(x_{\text{gal}}, y_{\text{gal}}, z_{\text{gal}}, U, V, W)$ (and more importantly their corresponding uncertainties). We use for this purpose the prescription Johnson & Soderblom 1987.

6.2. Motion in the galactic potential

The minimum LMA distances are useful at selecting the candidates but are a very crude approximation of the actual encounter conditions. This is especially true when the encounter time happens more than $\sim 10^5$ years in the past. In this case, the integrated effect of the galactic potential may modify substantially the position of the objects and the stars.

In order to obtain a “second order” estimation of the minimum distances, we need to integrate the trajectory of the surrogate objects and the stellar candidates in the galactic potential. Given the axisymmetric nature of the potential, we need to transform the cartesian coordinates of the objects with respect to the Sun $(x_{\text{gal}}, y_{\text{gal}}, z_{\text{gal}}, U, V, W)$ to cylindrical coordinates referred to the galactocentric reference system. Although this may seem a simple technical procedure, every detail counts when trying to avoid any source of additional uncertainties.

This coordinate transformation is achieved in three steps:

⁹ <http://github.com/seap-udea/iwander.git>

Catalog name	Number of objects	Hipparcos ID	Tycho-2 ID	CDS Code	Reference
Gaia DR1	2057050	93635	1963415	I/337/tgas	(1)
Hipparcos	117955	117955	–	I/239/hip_main	(2)
Tycho-2	1035445	–	1035445	I/259/tyc2	(2)
Simbad	118004	118004	–	–	(3)
Astro	2341261	24320	259824	–	This work
WEB1995	1167	494	673	III/213	(5)
GCS	16682	14955	–	J/A+A/530/A138	(6)
RAVE-DR5	520701	–	309596	III/279/rave_dr5	(7)
PULKOVO	35493	35493	–	III/252/table8	(8)
FAMAHEY2005	6690	6690	–	J/A+A/430/165/tablea1	(9)
BB2000	673	495	673	III/213	(10)
MALARODA	2178	866	2178	III/249/catalog	(11)
GALAH	10680	–	10680	J/MNRAS/465/3203	(12)
MALDONADO	495	495	0	J/A+A/521/A12/table1	(13)
RV	307525	36867	270658	–	This work
AstroRV	244589	37213	244589	–	This work

TABLE 2

CATALOGS USED TO COMPILE THE **AstroRV** CATALOG FOR THIS WORK. REFERENCES: (1) [BROWN ET AL. 2016](#), (2) [ESA 1997](#) (3) [WENGER ET AL. 2000](#), (5) [BARBIER-BROSSAT & FIGON 2000A](#), (6) [CASAGRANDE ET AL. 2011](#), (7) [KUNDER ET AL. 2017](#), (8) [GONTCHAROV 2006](#), (9) [FAMAHEY ET AL. 2005](#), (10) [BARBIER-BROSSAT & FIGON 2000B](#), (11) [MALARODA ET AL. 2000](#), (12) [MARTELL ET AL. 2016](#), (13) [MALDONADO ET AL. 2010](#).

1. Convert position and velocities referred to the local standard of rest (LSR) into position and velocities relative to the galactic center:

$$\vec{v}_{GC} = \vec{v}_{gal} + \vec{v}_{\odot} + v_{circ} \hat{y}_{gal}$$

$$\vec{r}_{GC} = \vec{r}_{gal} - R_{\odot} \hat{x}$$

where $\vec{v}_{gal} : (U, V, W)$ is the velocity of the star with respect to the Sun in galactic coordinates, $\vec{v}_{\odot} : (U_{\odot}, V_{\odot}, W_{\odot})$ is the velocity of the Sun with respect to the local standard of rest (LSR) and v_{circ} is the local circular velocity. In [Table 3](#) we show the values adopted for this quantities.

2. \vec{v}_{GC} and \vec{r}_{GC} are referred to a system pointing to the galactic center (the unprimed $x_{gal}, y_{gal}, z_{gal}$ in [Figure 3](#)). This system is rotated at an angle $\alpha = \sin^{-1}(z_{\odot}/R_{\odot})$ with respect to the plane of the Galaxy. Finally the physical galactocentric coordinates on which we must perform the orbital integration are obtained after the rotation:

$$\vec{r}'_{GC} = R_{\alpha} \vec{r}_{GC}$$

$$\vec{v}'_{GC} = R_{\alpha} \vec{v}_{GC}$$

with

$$R_{\alpha} = \begin{pmatrix} \cos \alpha & 0 & \sin \alpha \\ 0 & 1 & 0 \\ -\sin \alpha & 0 & \cos \alpha \end{pmatrix}$$

3. Express the galactocentric position and velocity in cylindrical coordinates $\vec{r}'_{GC} : (R, \theta, z)$, $\vec{v}'_{GC} : (\dot{R}, R\dot{\theta}, \dot{z})$.

In cylindrical coordinates, the equation of motion of an object moving in the potential of the galaxy $\Phi(R, \theta, z)$ are given by (see eg. [García-Sánchez et al. 2001](#)):

Property	Value	Reference
U_{\odot}	11.1 km/s	(1)
V_{\odot}	12.24 km/s	(1)
W_{\odot}	7.25 km/s	(1)
v_{circ}	220.0 km/s	(2)
z_{\odot}	27 km/s	(3)
R_0	8.3 kpc	(4)
M_d, a_d, b_d	$7.91 \times 10^{10} M_{\odot}, 3500pc, 250pc$	(5)
M_b, a_b, b_b	$1.40 \times 10^{10} M_{\odot}, 0, 350pc$	(5)
M_h, a_h, b_h	$6.98 \times 10^{11} M_{\odot}, 0, 24000pc$	(5)

TABLE 3

PROPERTIES OF THE GALAXY. REFERENCES: (1) [SCHÖNRICH ET AL. 2010](#), (2) [BOVY 2015](#), (3) [CHEN ET AL. 2001](#), (4) [BAILER-JONES 2015](#).

$$\begin{aligned} \ddot{R} &= -\frac{\partial \Phi}{\partial R} + R\dot{\theta}^2 \\ \ddot{\theta} &= -\frac{\partial \Phi}{\partial \theta} - 2\frac{\dot{R}\dot{\theta}}{R} \\ \ddot{z} &= -\frac{\partial \Phi}{\partial z} \end{aligned} \quad (4)$$

Here we assume for simplicity and axisymmetric Kuzmin-like potential for the three galactic subsystems ([Kuzmin 1956](#); [Miyamoto & Nagai 1975](#)), disk (d), bulge (b) and halo (h):

$$\Phi(R, \theta, z) = - \sum_{i=d,b,h} \frac{GM_i}{\sqrt{R^2 + (a_i + \sqrt{z^2 + b_i^2})^2}} \quad (5)$$

The value of the potential parameters M_i, a_i, b_i assumed for each component are summarized in [Table 3](#). Once the trajectory of the objects in the potential of the Galaxy are integrated we proceed to find the minimum distance of the nominal object to each of stellar candidate. This is a refined estimation of d_{min}, t_{min} .

To illustrate the differences between the LMA minimum distance and time and the same values obtained with precise integrations, we show in [Figure 5](#) curves of normalized relative distance between the 11/2017U1 nominal object and several surrogate stars corresponding to HIP 103749 (see below). We see that the quality

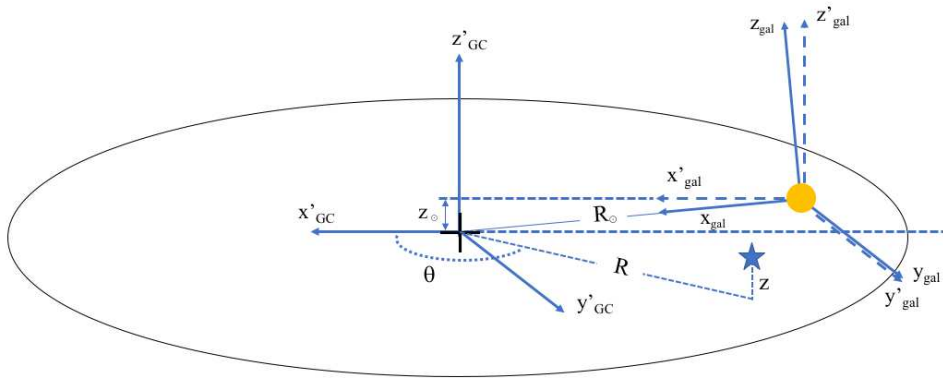


FIG. 3.— Galactic Reference Systems.

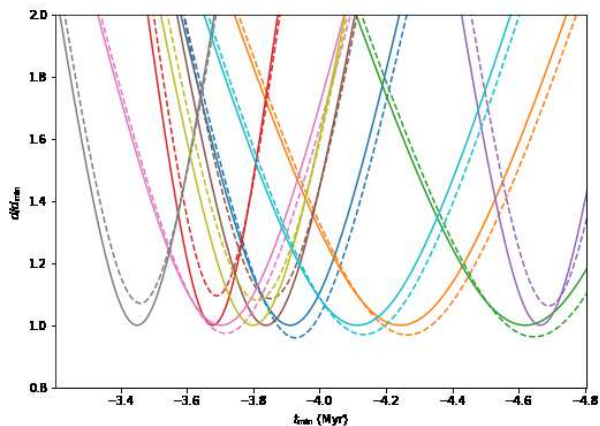


FIG. 4.— Periastron distances for different surrogate objects in the case of HD 200325.

of the LMA values depends on integration time and the specific trajectory of the star. Although in this case values of LMA d_{\min} are off by 5% – 10% from the precise one, we have seen cases where the differences are as large as 100%.

7. THE SURROGATE STARS

In the same way that we generate N_p surrogate objects to take into account the uncertainties in the orbit solution of the interstellar interloper, we generate, for each progenitor candidate, N_s “surrogate stars” with observed properties compatible with the nominal astrometric observables of the star, namely $(\alpha_0, \delta_0, \varpi_0, \mu_{\alpha,0}, \mu_{\delta,0})$. For this purpose we build a covariance matrix (see Equation 1) using the errors reported for each astrometric variable and their related correlations¹⁰.

In summary, studying with our method the coincidence in time and space of an interstellar object with a nearby star, implies dealing properly with this N_p surrogate objects flying close to N_s surrogate stars. Assessing the probability of a close encounter using just the nominal solutions for both, is unrealistic.

¹⁰ In the Hipparcos and Gaia databases, correlations are reported in the form of fields such as RA_DEC_CORR, RA_PARALLAX_CORR, etc.

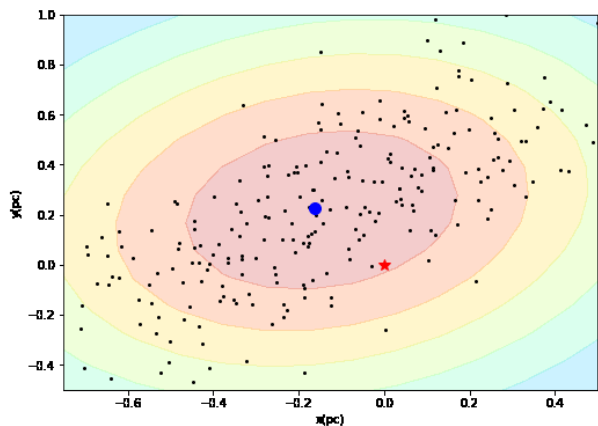


FIG. 5.— Scattering plot of the position of the surrogate objects at the time of minimum distance with the nominal star HD 200325 (red star). Contours show the number density of objects estimated with the methods in this work. The blue dot show the position of minimum distance assuming the nominal orbit.

8. INTERSTELLAR ORIGIN PROBABILITY

The question that originally motivates this work was how to compute the probability that a star with present astrometric properties $(\alpha, \delta, \varpi, v_r)$ has ejected in the past, a body that entered into the solar system with heliocentric orbital elements $(q, e, i, \Omega, \omega, t_p)$ at a given reference epoch t_0 .

If both, the astrometric position of a star and the orbital elements of the interstellar object were known with no uncertainties, the question could be answered by integrating backward the orbits of the object and the star, as described in the precedent section, and verifying if they coincide in space at some point in the past. However, with uncertain initial conditions assessing the probability is non-trivial. Even if the nominal trajectories of the object and the star do not coincide, there is a non-zero probability that they were actually related.

Let’s assume first that the astrometric information about the star is known with zero uncertainty. If we propagate all the surrogate objects until the time of minimum distance, t_{\min}^{nom} , the star will be surrounded by a cloud of points (see Figure 5), each one representing the position of the surrogate objects at that time. In the

continuous limit, even if none of the N_p surrogate objects coincide in position with the star, a probability different than zero exist that they were related. Our central assumption here is that the probability that such a relationship actually existed will be proportional to the density of surrogate objects at the position of the star.

Computing the number density from a discrete set of positions of the surrogate objects, is challenging. Several numerical techniques have been devised and applied in other areas such as cosmology and hydrodynamics (see eg. [Price 2012](#)), to asses similar problems. More recently, [Zuluaga & Sucerquia 2017](#) applied the approach used in Smooth Particle Hydrodynamics in the context of impact probabilities in the the Solar System. According to this approach the number density of trajectories around the star can be computed as:

$$n(\vec{r}_*) = \sum_i^{N_s} W(|\vec{r}_* - \vec{r}_i|, h) \quad (6)$$

where $|\vec{r} - \vec{r}_i|$ is the distance between the star and the i th surrogate object, h is a distance-scale for the distribution, and $W(d, h)$ is called a *smoothing kernel*. In this work we use for h , the characteristic size of the surrogate object cloud at the time of minimum approach. Other prescriptions can be used, but for the purpose of testing our method we will restrict to this simple ansatz.

Different kernel function can be used to calculated n . Although it is common to use a *B-spline kernel* (see eg. [Zuluaga & Sucerquia 2017](#)), for the purposes pursued here, the best suited function is one that provide non-zero, although still very low values for $n(r_*)$ at large values of $|\vec{r}_* - \vec{r}_i|$. The chosen kernel function is ([Price 2012](#)):

$$W(d, h) = \sigma \exp(-d^2/h^2) \quad (7)$$

where σ is a normalization constant.

The probability that the interstellar object be at t_{\min}^{nom} inside a small volume dV around the star position will be given by:

$$p(r_*)dV = \frac{n(r_*)dV}{N_p}$$

In the discrete case, if we take ΔV as a fixed small enough volume, the probability of a coincidence in position, P_{pos} between star at r_* an the interstellar object (within the volume ΔV) will be:

$$P_{\text{pos}} \approx \frac{n(r_*)\Delta V}{N_p} \quad (8)$$

this is assuming that $n(r)$ does not change significantly inside ΔV . We will assume, arbitrarily, ΔV as the volume inside the truncation radius of a solar-mass star, i.e. $\Delta V \approx (4\pi/3)0.5^3 \text{ pc}^3 \approx 0.5 \text{ pc}^3$. Of course the final IOP will depend on the particular election of the free parameters of our model, eg. h , ΔV . However if these values are the same for all stars in the analysis, the conclusion from the comparison of probabilities will be the same.

Now, if we admit that the position of the star at the point of minimum distance is also uncertain and repeat the preceding computation for each of the N_s surrogate

stars, the joint probability that the interstellar object intersected the star at t_{\min}^{nom} can be estimated as,

$$P_{\text{pos}} \approx \frac{1}{N_s} \sum_i P_{\text{pos},i}$$

The fact that the position of the object and the star coincide in space does not guarantee that the object be ejected from an hypothetical planetary system around it. If II/2017U1 reaches another stellar system in the future, their inhabitants may think that the Solar System is the progenitor of the object.

There are actually two additional factors constraining the origin probability: the relative velocity, the stellar distance and the previous encounters with other stars.

8.1. Relative velocity

Only a few processes may lead to the ejection of a small body from an almost-isolated planetary system ([Melosh 2003](#); [Napier 2004](#)). In the low density solar neighborhood the more feasible ejection mechanisms are the particle-particle gravitational scattering, where small bodies receive a gravitational slingshot effect after encountering a planet, at the right conditions ([Wiegert 2014](#)).

We estimate the distribution of excess velocities, v_{∞} , that small bodies (asteroids and comets) receive from their encounters with a giant planet around a solar mass star, using a semianalytical approach inspired in the works by [Wiegert \(2011, 2014\)](#).

For this purpose, we first set up a planetary system having a single planet of mass M_p located in a circular orbit with semimajor axis a_p . We randomly generate orbital elements for small bodies such that they intersect the orbit of the planet. For simplicity the small-body semimajor axis, eccentricity and orbital inclinations were uniformly generated in the whole range of possible values, eg. $a \in (0.5a_p - 1.5a_p)$, $e \in (0, 1)$, $i \in (0, 90)$ deg. Longitude of ascending node and argument of periapsis were calculated imposing the condition that the small body and the planet collide.

For each planet-small body orbit configuration we compute the relative velocity with which they encounter and the direction with respect to the planet reference frame from which the small body approaches. From here we follow the prescription of [Wiegert \(2011\)](#) to compute the outbound velocity of the object after interacting with the planet. A random position (x_p, y_p) over the tangent plane to the Hill sphere is generated (see Figure 1 in [Wiegert 2014](#)). From there we compute the impact parameter, scattering angle, planetocentric orbital eccentricity and periapsis distance. Finally we rotate the planetocentric inbound velocity to compute the outbound velocity of the small-body at the Hill radius with respect to the planet and then with respect to the star.

Once the synthetic small bodies in our simulation are scattered by the planet, we evaluate if their outbound velocity v with respect to the star is larger than the escape velocity v_{esc} at the position of the planet. If this is the case, we compute the excess velocity, $v_{\text{inf}}^2 = v^2 - v_{\text{esc}}^2$.

In [Figure 6](#) we show the distribution of excess velocities resulting from the interactions of small bodies with planets of different mass M_p located in a circular orbit $a_p = 5$ AU around a solar mass-star. The results are given in

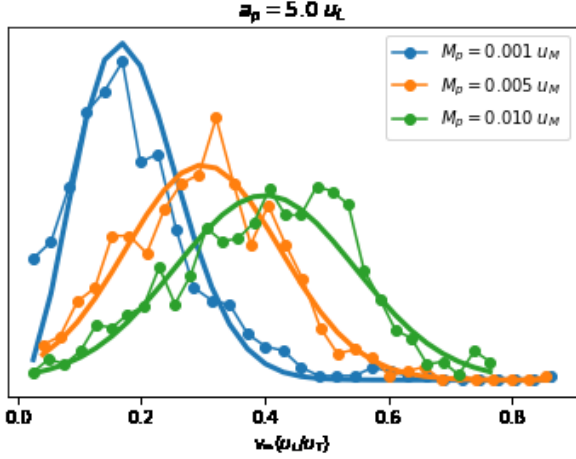


FIG. 6.— Ejection velocity distribution for a planet in a circular orbit at $a_p = 5 u_L$ and different planetary masses. Continuous thick lines are Maxwell-Boltzmann distributions with the same mean as the numerical results.

canonic units for which we have set $G = 1$, $u_L = 1$ AU and $u_M = 1 M_\odot$. In these units, $u_T = \sqrt{u_L^3 / (G u_M)}$, and $u_L / u_T = 30$ km/s.

An interesting advantage of expressing the results in canonic units is that they can be used to predict ejection velocities distribution from planetary systems around stars of arbitrary mass. Thus, for instance, the average escape velocity for a planet with the mass of Jupiter around a solar mass star, $u_M = 1 M_\odot$, $M_p = 0.001 u_M$ is $\bar{v}_\infty = 0.2 u_L / u_T$, or 6 km/s (see the leftmost curve in Figure 6). If we consider now a late M-dwarf with mass $M_\star = 0.5 M_\odot$, the same results in Figure 6 will apply, but now for the case of a planet with half the mass of Jupiter located at $5 u_L$ from the star. The value of \bar{v}_∞ in km/s, will depend on what value assumed for u_L . If we take $u_L = 1$ AU (as in the case of the solar-mass star), then $u_L / u_T = 20$ km/s for the late M-dwarf, and the average ejection velocity will be 4 km/s.

In Figure 7 we show contours of \bar{v}_∞ in the $a_p - M_p$ plane. We discover that for masses below $10^{-3} u_M$ ejection velocities are only a function of planetary orbital distance and are very insensitive to planetary mass.

Another interesting result from our semi analytical experiments is that the ratio of the standard deviation σ_{v_∞} to the mean value of of the ejection velocity \bar{v}_∞ , is almost independent of planetary orbital distance. In Figure 8 we show a plot of the value of $\sigma_{v_\infty} / \bar{v}_\infty$ for different planetary masses. It is interesting to notice that in the case of a Maxwell-Boltzmann distribution (MBD) the ratio σ / μ (with μ the mean) is constant and equal to 0.42 which is of the order of $\sigma_{v_\infty} / \bar{v}_\infty$. This seems to suggest that the ejection velocities can be fitted by a MBD with a mean that depends on M_p and a_p . This is precisely the fitting functions we have used in Figure 6.

Using the average ejection velocities in Figure 7 and the dispersion-to-mean ratio in Figure 8, we can estimate the velocity distribution of small-bodies being ejected from a planetary system around a star of a given mass. Since ejection velocities depend on the unknown mass M_p and semimajor axis a_p of the largest planet in the system, we estimate the “posterior” ejection velocity probabili-

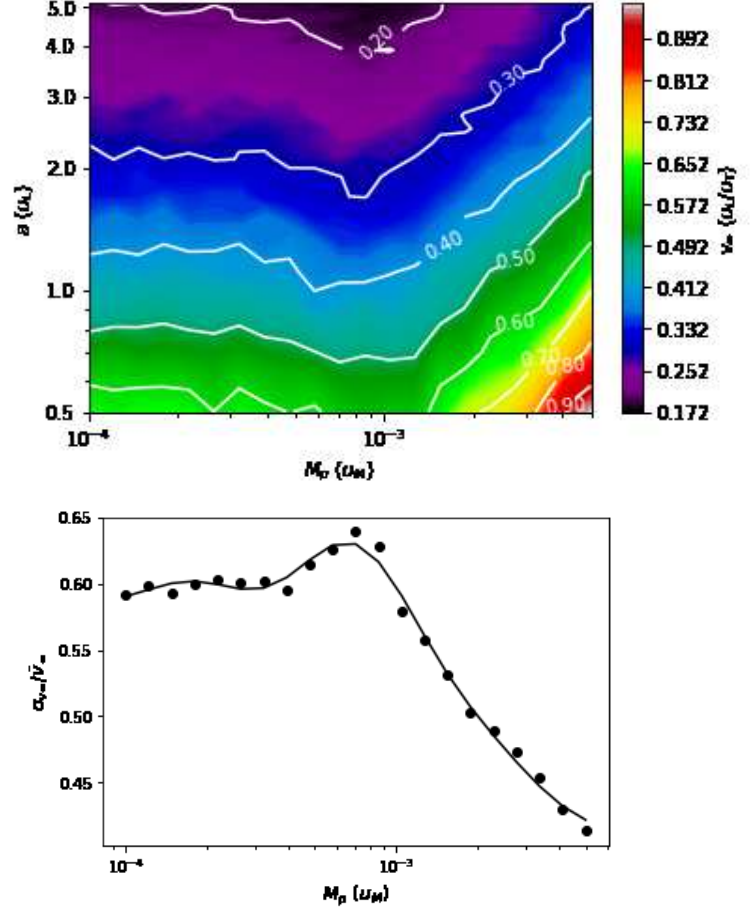


FIG. 7.— Upper panel: ejection mean velocity for different planetary masses and orbital sizes. Lower panel: ratio of the average to the standard deviation of the ejection velocities for different planetary masses. Properties are given in canonic unites. If $u_L = 1$ AU and $u_M = 1 M_\odot$, $u_v = u_L / u_T = 30$ km/s.

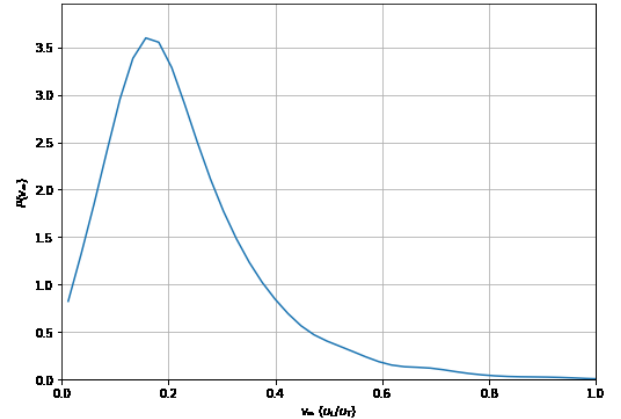


FIG. 8.— Ejection velocity posterior distribution as estimated in this work.

ties, assuming for simplicity uniform “priors” for these quantities. The resulting posterior distribution $p_{v\infty}(v)$ for the case of a solar-mass star is shown in ??.

The probability that an interstellar object be ejected from a star with relative velocity between v_{rel} and $v_{\text{rel}} + \Delta v$ is estimated as:

$$P_{\text{vel}} \approx p_{v\infty}(v_{\text{rel}})\Delta v$$

In our model, we take for Δv the value of the velocity dispersion in the cloud of surrogate objects.

8.2. Stellar distance

If we assume that objects are ejected isotropically from the planetary system (as suggested in the Solar System from the geometry of the Oort cloud, see e.g. [Emel’Yanenko et al. 2007](#) and references therein), we can estimate the probability that an ejected object crosses the Solar truncation radius $R_{\text{T},\odot}$ while the star is at a distance d_* :

$$P_{\text{dis}} = \left(\frac{R_{\text{T},\odot}}{d} \right)^2$$

8.3. Previous encounters

A single surrogate object in our simulations may suffer multiple encounters with nearby stars. Thus, for instance, while evaluating the probability that the object be ejected from Star 1 at t_1 , it could exist a Star 2 from which the object could be ejected at a posterior time t_2 , ie. $t_2 > t_1$. If this is the case, the probability that the object be ejected from Star 1 should be weighted by the probability of be ejected from Star 2. If we sort the potential progenitors in inverse chronological order (first the more recent), the weighting factor, or the previous encounter probability will be given by:

$$P_{\text{enc},i} = \prod_{t_j > t_i} (1 - P_{\text{IOP},j}) \quad (9)$$

where $P_{\text{IOP},j}$ is the interstellar origin probability computed for j th star. Thus, we would be preferring recent ejections over earlier ones.

With all these elements at hand the interstellar origin probability of a given object will be:

$$P_{\text{IOP}} = P_{\text{pos}}P_{\text{vrel}}P_{\text{dis}}P_{\text{enc}} \quad (10)$$

9. RESULTS

As an illustrative example (not necessarily the better, but the only to date), we apply our methodology to asses the interstellar origin of 1I/2017U1. In [Table 4](#) we present a list of the progenitor candidates satisfying $t_{\text{min}}^{\text{nom}} < 10^7$ years, with their respective IOP probabilities.

The method presented here does not necessarily intend to identify a single object as the actual progenitor of 1I/2017U1. Finding the origin would require follow-up observations of the interstellar object (while reachable), and improving the astrometric properties of the candidate star. When more and better information be available about these and other stars the list could

be extended or reduced, and more importantly the IOP probability could be modified.

Still, it is interesting to notice the properties of several of these candidates. We have highlighted those stars for which the interval of minimum distances is not too wide (in several cases minimum distances may span intervals two orders of magnitude wide, eg. TYC 5781-1104-1 and TYC 8821-119-1). We are also interested on those stars that with the available information has minimum closest approaches below 1 pc.

The most interesting case is of course that of HD 200325 (HIP 103749), the first object in the list. The star is probably actually a double or multiple system. The system is located at the present at a distance of 52 pc from the Sun. The object has been well studied (see eg. [Cvetković 2011](#); [Holmberg et al. 2007](#)) and their physical properties are well constrained. Its radial velocity has been measured very precisely ($v_r = -11.10 \pm 0.4$ km/s) and their astrometric properties comes from the Hipparcos mission. The object, however, is not included in the Gaia DR1. As a result its proper motion, especially in declination, is known with a poor uncertainty ($\mu_{\text{dec}} = 0.90 \pm 0.60$ mas). This is probably the reason why the minimum distance has such a large uncertainty, ie. (0.1-6-6) pc. The mass of the main component of the System is $1.19 \pm 0.1 M_{\odot}$, and its age is 3.2 Gyr. The companion seems to be a low mass K-dwarf ([Cvetković 2011](#)) located at ~ 25 AU from the primary. Although no planet has been discovered yet around the primary star, and its binary nature may prevent the formation of giant planets ([Thebault 2011](#)), the stars are far apart and their masses are very dissimilar. Interestingly there is a known binary system with similar characteristics, HD 41004 (a solar mass evolved primary with a low-mass companion at 20 AU) around which a jupiter-mass planet has been discovered at ~ 1 AU from the primary ([Zucker et al. 2004](#)). The existence of this “doppelgänger”, together with recent theoretical evidence that shows that formation of planets around this kind of binaries could not be as improbable as thought ([Higuchi & Ida 2017](#)), lead us to speculate that it our candidate HD200325 may have a planetary system and probably be the source of ejected small bodies.

Of course it is too early to conclude that 1I/2017U1 comes actually from our best candidate. We expect that improved astrometric information about the star released with Gaia DR2, help us to improved the IOP for this and other candidates.

10. DISCUSSION

When dealing with very uncertain processes such as those involved in this problem, it is important to ask if the identified close encounters could be just the product of chance. Further numerical experiments should be performed to test this idea and will be presented in a companion paper.

At least two groups, that of [Portegies Zwart et al. \(2017\)](#) and [Dybczyński & Królikowska \(2017\)](#) published their own list of candidates. None of their objects, however, were included in the preliminary list in [Table 4](#).

We searched for those objects among our *AstroRV* catalog and find that either some of them candidates were not included in our input catalog or have properties (relative velocities, time for minimum approach) too large

ID		Nominal			Range			log P			
HIP/TYCHO	Other	t_{\min} Myr	d_{\min} pc	v_{rel} km/s	t_{\min} Myr	d_{\min} pc	v_{rel} km/s	$\langle P_{\text{pos}} \rangle$	$\langle P_{\text{vel}} \rangle$	P_{dist}	IOP
HIP 103749	HD 200325	-3.9	0.6	12	[-4.9, -3.3]	[0.1, 6.6]	[10, 14]	-3.4	-2.5	-4.1	-7.4
HIP 17288	HD 23121	-6.7	5.5	15	[-7.1, -5.8]	[1.5, 16.7]	[14, 16]	-4.7	-2.7	-4.6	-9.3
TYC 6988-276-1	-	-6.0	6.8	17	[-7.4, -4.8]	[0.1, 53.4]	[14, 20]	-4.9	-2.9	-4.7	-9.5
HIP 43100	* iot Cnc B	-6.0	10.7	17	[-7.6, -4.0]	[1.3, 21.9]	[13, 21]	-5.8	-3.5	-4.7	-10.5
TYC 6961-156-1	-	-7.9	6.5	24	[-8.4, -6.9]	[0.6, 40.9]	[23, 25]	-6.3	-4.3	-5.2	-11.4
HIP 97022	HD 186159	-2.4	7.5	23	[-3.0, -1.9]	[0.8, 12.2]	[20, 26]	-6.4	-4.1	-4.2	-10.7
HIP 77570	HD 141693	-8.1	14.4	13	[-9.8, -5.8]	[3.8, 65.9]	[10, 17]	-6.6	-2.6	-4.8	-11.3
TYC 9523-1571-1	-	-3.9	1.4	34	[-4.7, -3.5]	[0.1, 9.8]	[29, 38]	-7.0	-5.9	-4.9	-11.9
HIP 83532	HD 155262	-5.2	6.1	19	[-5.9, -4.5]	[2.7, 10.5]	[17, 22]	-7.2	-3.6	-4.7	-11.9
HIP 63797	HD 113376	-2.9	0.7	40	[-3.4, -2.7]	[0.1, 5.9]	[36, 44]	-7.2	-6.6	-4.8	-12.0
TYC 5222-131-1	-	-8.1	31.5	29	[-9.9, -6.1]	[1.4, 315.7]	[25, 45]	-7.2	-5.0	-5.5	-12.5
HIP 10519	HD 13759	-7.3	11.5	25	[-8.5, -6.4]	[3.2, 40.9]	[22, 27]	-7.4	-4.2	-5.2	-12.5
TYC 6187-522-1	-	-9.9	9.2	26	[-12.3, -8.1]	[1.7, 74.6]	[20, 35]	-7.5	-4.8	-5.5	-13.0
HIP 23744	HD 32684	-7.7	7.4	18	[-12.5, -5.7]	[5.3, 23.1]	[11, 24]	-7.8	-4.7	-4.9	-12.7
TYC 5172-2349-1	-	-4.6	4.3	35	[-5.5, -3.9]	[1.4, 20.8]	[30, 40]	-8.1	-5.9	-5.1	-13.2
HIP 96423	HD 184853	-7.2	14.8	34	[-10.0, -5.9]	[2.1, 82.5]	[31, 39]	-8.4	-5.4	-5.4	-13.8
TYC 7604-5-1	-	-4.5	4.2	40	[-7.0, -3.6]	[0.9, 17.4]	[25, 49]	-8.4	-6.1	-5.2	-13.6
TYC 5855-2215-1	-	-6.6	4.0	40	[-7.9, -5.2]	[0.8, 121.5]	[39, 48]	-8.9	-6.5	-5.5	-14.3
HIP 102170	HD 197274	-5.9	6.0	36	[-6.7, -5.4]	[3.3, 12.3]	[35, 36]	-9.0	-5.8	-5.3	-14.4
TYC 5781-1104-1	-	-7.5	31.4	38	[-9.3, -5.8]	[1.6, 224.1]	[35, 45]	-9.0	-5.8	-5.5	-14.5
TYC 8821-119-1	-	-8.8	31.5	43	[-11.7, -6.5]	[0.5, 229.3]	[35, 60]	-9.1	-6.9	-5.9	-14.7
TYC 5617-986-1	-	-7.9	8.1	45	[-9.8, -6.3]	[0.2, 82.5]	[40, 53]	-9.1	-7.2	-5.7	-14.8
HIP 17980	HD 23897	-9.1	11.5	33	[-12.2, -6.5]	[4.0, 72.8]	[30, 38]	-9.2	-5.9	-5.6	-14.8
HIP 15928	HD 21142	-4.0	9.4	26	[-4.9, -3.3]	[3.4, 29.4]	[23, 29]	-9.5	-4.6	-4.7	-14.2
HIP 18453	* 43 Per	-0.9	1.0	41	[-1.0, -0.8]	[0.5, 5.1]	[41, 43]	-9.5	-6.6	-3.8	-13.4
TYC 5510-322-1	-	-6.3	4.7	44	[-7.8, -4.7]	[2.0, 212.6]	[39, 52]	-9.6	-7.1	-5.7	-15.1
TYC 4666-72-1	-	-8.0	39.0	48	[-9.5, -5.3]	[0.9, 702.1]	[44, 85]	-9.6	-8.0	-5.9	-15.3
HIP 109639	HD 210601	-7.1	10.0	11	[-8.2, -6.4]	[7.1, 15.6]	[10, 12]	-9.8	-2.3	-4.4	-14.3
TYC 7961-612-1	-	-9.7	44.0	32	[-11.0, -8.0]	[5.5, 214.5]	[29, 37]	-10.0	-5.6	-5.7	-15.5
HIP 117133	HD 222932	-5.2	13.0	26	[-6.9, -4.3]	[4.1, 38.5]	[25, 29]	-10.0	-4.5	-4.9	-15.0

TABLE 4
INTERSTELLAR ORIGIN PROBABILITY (IOP) FOR A SELECTED GROUP OF NEARBY STARS.

for our particular selection criteria. This fact put in evidence a limitation of any approach to assess the origin of an interstellar object: the database completeness.

It is interesting to notice, however that we have verified that at least the most promising candidate in [Dybczyński & Królikowska \(2017\)](#), namely TYC 5325-1808-1, was also identified in our preliminary filtering process. More interestingly, the reported minimum distance and time of closest approach coincide with our own estimations. However, the time of closest approach for this object is larger than our limit of 10 Myr, a time when the cloud of surrogate objects has expanded to a size comparable to the average distance among stars in the solar neighborhood.

The approach presented here to estimate ejection velocities of small bodies from planetary system, is only our first attempt to model what could be a more complex problem. Although a lot of interest have been paid in to model the flux of planetesimals coming out from young planetary systems, predicting the direction and velocities of these ejected objects has received less attention. The case of interstellar objects and the investigation of their origin could encourage more investigation in this field. Thus, for instance, improved semi-analytical models and detailed numerical n-body simulations may be required to better constraint the kinematical properties of ejected small bodies from already formed planetary systems around single and multiple stellar systems. We have already performed several basic n-body simulations to investigate the problem that confirm some of our semi-analytical results but seem to predict lower ejection ve-

locities in some regions of the parameter space.

Although trillions of interstellar small objects are wandering around the Solar System and most of them could be there for hundreds of millions if not billions of years, the effort for tracing back the origin of some of those that come for chance into the inner Solar System is not irrelevant. Although many stars may have contributed in the history of Galaxy to populate this graveyard, of course nearby stellar system could be an important source of many of these objects.

Assessing the origin of interstellar objects require that small uncertainties in the initial kinematical parameters do not propagate into large errors in the resulting dynamical properties due to factors related with the simulation process. Some sources of errors include but are not restricted to galactic coordinate transformation, uncertainties in the galactic parameters and of course errors in coding and processing the data.

In the same way as the trajectory can be propagated backward, it could also be propagated forward in time.

11. SUMMARY AND CONCLUSIONS

In this paper we presented a general method for calculating the probability that nearby stars be the source of an interstellar small object detected inside the Solar System. The method rely on the availability of a precisely determined orbit for the object and precise astrometric information about a large enough number of nearby stars. For illustrating the method we apply it for assessing the origin of 1I/2017U1, the first interstellar object.

The application of our method to the case of 1I/2017U1 allowed us to identify a handful of stars whose kinemati-

cal and physical properties are compatible with the ejection of a small object in the latest couple of Myrs. Of particular interest, at least with the available information is the binary(multiple) system HD200325. The system is dominated by a primary star $1.2 M_{\odot}$ with a K-dwarf companion at ~ 25 AU. Although planetary systems have been discovered around the primary or the secondary star, several similar multiple systems have been discovered in the past with planets, making the case for HD200325 not as unlikely as initially thought.

Our method is not intended to identify a single object. Even with small uncertainties in the initial orbit and in the astrometric position of the stars, there always will be large enough uncertainties in the resulting kinematical properties that constrained our capability to pinpoint a single source. The aim is to identify stars whose properties could be studied in more detail to reduce the uncertainties and increase/decrease the probability that they can be the sources of these objects.

One of the most interesting application of our method is that IOP probabilities can be published and updated permanently when new and better information be obtained. A catalog of candidate objects for this and other

future discovered interstellar objects can also be compiled and published with a global ranking of IOP probabilities. The authors believe that it could be a time in the future when this and other efforts allows us to pinpoint precisely the provenance of an interstellar object. This will be the times when instead of going to other planetary systems we can study them using natural probes approaching to the Solar System.

ACKNOWLEDGEMENTS

We thank Cory Bailer-Jones for providing some of the data used in this work to compile the AstroRV catalog. We have used NASA's ADS Bibliographic Services. Most of the computations that made possible this work were performed with Python 2.7 and their related tools and libraries, iPython (Pérez & Granger 2007), Matplotlib (Hunter et al. 2007), scipy and numpy (Van Der Walt et al. 2011). This work has made use of data from the European Space Agency (ESA) mission *Gaia* (<https://www.cosmos.esa.int/gaia>), processed by the *Gaia* Data Processing and Analysis Consortium (DPAC, <https://www.cosmos.esa.int/web/gaia/dpac/consortium>).

APPENDIX

We have provided with this work an open source package, *iWander*, that implements the general methodology described here. Providing a fully fledged computational tool is not only an effort to make these results reproducible, but also to allow the methodology to be applied by any researcher once future interstellar objects are discovered. The package can also serve as a basis or an inspiration to develop better computational tools for this and other related problems.

To the date this manuscript was prepared, the documentation of the package is still under preparation. Here we provide some basic information about the package that can be useful for users and developers:

- The package is available at GitHub: <http://github.com/seap-udea/iWander>.
- The required NASA NAIF SPICE kernels as well as the libraries required to compile them, are provided with the package while complying the corresponding licenses, in order to ease its compilation and use.
- The core modules of the package were written in C/C++ to guarantee computing efficiency. As a result they should be compiled before usage. Other post processing modules were written in Python and are provided as core python scripts as well as iPython notebooks.
- One of the key components of the methodology and the package are the astrometric and radial velocities catalogs. Although all of them are publicly available we also provide them with the package. This is to allow the developer trying different merging and filtering strategies when compiling the input AstroRV catalog.
- The version of the AstroRV catalog used in this work is also provided with the package. As a result, the full size of the local copy is almost 3 GB in size. A smaller size version of the package with a size of only 450 MB is available at <http://github.com/seap-udea/iWander>.
- Any contribution to the development of the package is welcomed. We can provide full access to the developing branch to any researcher or developer interested in to contribute with this project.
- The package, as well as the related databases will be updated as future and best astrometric and radial velocity information be published.

REFERENCES

- Acton Jr, C. H. 1996, *Planetary and Space Science*, 44, 65
 Adams, F. C., & Spiegel, D. N. 2005, *Astrobiology*, 5, 497
 Bailer-Jones, C. 2017, *Astronomy & Astrophysics*
 Bailer-Jones, C. A. L. 2015, *A&A*, 575, A35
 Barbier-Brossat, M., & Figon, P. 2000a, *Astronomy and Astrophysics Supplement Series*, 142, 217
 —. 2000b, *Astronomy and Astrophysics Supplement Series*, 142, 217
 Belbruno, E., Moro-Martín, A., Malhotra, R., & Savransky, D. 2012, *Astrobiology*, 12, 754
 Berski, F., & Dybczyński, P. A. 2016, *A&A*, 595, L10
 Bolin, B. T., Weaver, H. A., Fernandez, Y. R., et al. 2017, *ArXiv e-prints*
 Bovy, J. 2015, *The Astrophysical Journal Supplement Series*, 216, 29

- Brown, A. G., Vallenari, A., Prusti, T., et al. 2016, *Astronomy & Astrophysics*, 595, A2
- Bulirsch, R., & Stoer, J. 1966, *Numerische Mathematik*, 8, 1
- Casagrande, L., Schoenrich, R., Asplund, M., et al. 2011, *Astronomy & Astrophysics*, 530, A138
- Chambers, K. C., Magnier, E. A., Metcalfe, N., et al. 2016, ArXiv e-prints
- Chen, B., Stoughton, C., Smith, J. A., et al. 2001, *The Astrophysical Journal*, 553, 184
- Cvetković, Z. 2011, *The Astronomical Journal*, 141, 116
- de la Fuente Marcos, C., & de la Fuente Marcos, R. 2017, *Research Notes of the American Astronomical Society*, 1, 5
- Dybczyński, P. A., & Królikowska, M. 2017, ArXiv e-prints
- Emel'Yanenko, V. V., Asher, D. J., & Bailey, M. E. 2007, *MNRAS*, 381, 779
- Engelhardt, T., Jedicke, R., Vereš, P., et al. 2017, *AJ*, 153, 133
- ESA, ed. 1997, *ESA Special Publication*, Vol. 1200, *The HIPPARCOS and TYCHO catalogues. Astrometric and photometric star catalogues derived from the ESA HIPPARCOS Space Astrometry Mission*
- Famaey, B., Jorissen, A., Luri, X., et al. 2005, *A&A*, 430, 165
- Ferrin, I., & Zuluaga, J. 2017, ArXiv e-prints
- Gaidos, E., Williams, J., & Kraus, A. 2017, *Research Notes of the American Astronomical Society*, 1, 13
- Galassi, M., Davies, J., Theiler, J., et al. 2002, *Network Theory Ltd*, 3
- García-Sánchez, J., Weissman, P. R., Preston, R. A., et al. 2001, *A&A*, 379, 634
- Gontcharov, G. A. 2006, *Astronomy Letters*, 32, 759
- Gragg, W. B. 1965, *Journal of the Society for Industrial and Applied Mathematics, Series B: Numerical Analysis*, 2, 384
- Higuchi, A., & Ida, S. 2017, *The Astronomical Journal*, 154, 88
- Høg, E., Fabricius, C., Makarov, V. V., et al. 2000, *A&A*, 355, L27
- Holmberg, J., Nordström, B., & Andersen, J. 2007, *Astronomy & Astrophysics*, 475, 519
- Hunter, J. D., et al. 2007, *Computing in science and engineering*, 9, 90
- Ivezic, Z., Tyson, J. A., Abel, B., et al. 2008, ArXiv e-prints
- Jewitt, D., Luu, J., Rajagopal, J., et al. 2017, ArXiv e-prints
- Johnson, D. R., & Soderblom, D. R. 1987, *The Astronomical Journal*, 93, 864
- Kunder, A., Kordopatis, G., Steinmetz, M., et al. 2017, *The Astronomical Journal*, 153, 75
- Kuzmin, G. 1956, *Astronomicheskii Zhurnal*, 33, 27
- Malaroda, S., Levato, H., Morrell, N., et al. 2000, *A&AS*, 144, 1
- Maldonado, J., Martínez-Arnáiz, R. M., Eiroa, C., Montes, D., & Montesinos, B. 2010, *A&A*, 521, A12
- Mamajek, E. 2017, ArXiv e-prints
- Martell, S., Sharma, S., Buder, S., et al. 2016, *Monthly Notices of the Royal Astronomical Society*, stw2835
- Masiero, J. 2017, ArXiv e-prints
- McGlynn, T. A., & Chapman, R. D. 1989, *ApJ*, 346, L105
- Melosh, H. J. 2003, *Astrobiology*, 3, 207
- Merlin, F., Hromakina, T., Perna, D., Hong, M. J., & Alvarez-Candal, A. 2017, *A&A*, 604, A86
- Miyamoto, M., & Nagai, R. 1975, *Publications of the Astronomical Society of Japan*, 27, 533
- Napier, W. M. 2004, *MNRAS*, 348, 46
- Opik, E. 1932, *The Scientific Monthly*, 35, 109
- Pérez, F., & Granger, B. E. 2007, *Computing in Science & Engineering*, 9, 21
- Perryman, M. A. C., Lindgren, L., Kovalevsky, J., et al. 1997, *A&A*, 323, L49
- Portegies Zwart, S., Pelupessy, I., Bedorf, J., Cai, M., & Torres, S. 2017, ArXiv e-prints
- Price, D. J. 2012, *Journal of Computational Physics*, 231, 759
- Schönrich, R., Binney, J., & Dehnen, W. 2010, *Monthly Notices of the Royal Astronomical Society*, 403, 1829
- Sen, A. K., & Rama, N. C. 1993, *A&A*, 275, 298
- Strom, R. G., Malhotra, R., Ito, T., Yoshida, F., & Kring, D. A. 2005, *Science*, 309, 1847
- Strom Robert, G., Renu, M., Zhi-Yong, X., et al. 2015, *Research in Astronomy and Astrophysics*, 15, 407
- Thebault, P. 2011, *Celestial Mechanics and Dynamical Astronomy*, 111, 29
- Trilling, D. E., Robinson, T., Roegge, A., et al. 2017, ArXiv e-prints
- Van Der Walt, S., Colbert, S. C., & Varoquaux, G. 2011, *Computing in Science & Engineering*, 13, 22
- Wenger, M., Ochsenbein, F., Egret, D., et al. 2000, *A&AS*, 143, 9
- Wiegert, P. A. 2011, in *Meteoroids: The Smallest Solar System Bodies*, ed. W. J. Cooke, D. E. Moser, B. F. Hardin, & D. Janches, 106
- Wiegert, P. A. 2014, *Icarus*, 242, 112
- Ye, Q.-Z., Zhang, Q., Kelley, M. S. P., & Brown, P. G. 2017, ArXiv e-prints
- Zucker, S., Mazeh, T., Santos, N., Udry, S., & Mayor, M. 2004, *Astronomy & Astrophysics*, 426, 695
- Zuluaga, J. I., Ferrin, I., & Geens, S. 2013, ArXiv e-prints
- Zuluaga, J. I., & Sucerquia, M. 2017, in *Revista Mexicana de Astronomia y Astrofisica Conference Series*, Vol. 49, *Revista Mexicana de Astronomia y Astrofisica Conference Series*, 79–79